

Influence of the deposition time and temperature on the texture of InN thin films grown by RF-magnetron sputtering

L. BRAIC*, N. C. ZOITA

National Institute for Optoelectronics, P.O.Box MG-5, RO 077125, Bucharest, Romania

Indium nitride is an attractive semiconductor material for optoelectronic applications, high-speed electronics and solar cells. We report successful deposition of polycrystalline InN thin films onto un-etched plain (100) Si substrates by reactive RF magnetron sputtering method. The crystallographic characterization data and band-gap values are presented in relation with the films' growth temperature and deposition time.

(Received November 22, 2010; accepted November 29, 2010)

Keywords: Indium nitride, Growth temperature, Crystalline structure, Band-gap, RF-magnetron sputtering

1. Introduction

The fundamental parameters of InN films, including the band-gap and lattice constants exhibit values spanning a wide range, which are not yet fully understood. From the report of Tansley and Foley [1], the fundamental band gap energy of hexagonal InN was assigned to be around 1.9 eV, till recently, when the corroborate photoluminescence (PL) and optical absorption measurement [2]-[4] pointed for the revision of bandgap energy from ~ 1.9 eV to the lower value ~ 0.7 eV.

Besides the hexagonal III-V nitrides (gallium nitride GaN, aluminum nitride AlN), also indium nitride (InN) has been extensively studied in the recent period due to its wide applications in optoelectronic devices, including low-cost solar cells with high efficiency, optical coatings, and various types of sensors [5]. Due to its lower band gap, as compared to GaN and AlN, the resulting alloys may be the key for the fabrication of InGaAlN based short-wavelength semiconductor laser diodes [6]-[8]. Also, recent studies showed that InN and other III-V nitrides are promising materials for Terahertz radiation generation [9]-[12]. The emerging application of InN in microwave transistor devices, depends on its band-gap, with higher values being preferable. Alternately, if the band-gap of InN is smaller, then the applications in full spectrum solar cells based on InGaN hold considerable promise. So, it is necessary to have reproducible methods for the production of each type of InN film, as specific applications are readily available.

One early observed characteristic of InN is its lattice mismatch with the commonly used monocrystalline substrates, so that for high quality films a buffer layer is necessary, hexagonal AlN or GaN being usually used [13]. Even if the growth mode of most semiconductor thin films, and hence their properties, are determined by the characteristics of the substrate, InN seems to also display

its unique and valuable properties in unusual conditions, when grown without any buffer layer, directly on Si [14] or flexible kapton [15] substrates. If cost-effective InN based devices could be developed, using low cost substrates, it would open interesting possibilities for many applications.

In the reactive sputtering of semiconductor thin films, a higher growth temperature improves the crystallinity by increasing the ad-atoms energy and thus mobility. This allows them to occupy positions of lower energy, increases the surface and volume diffusion rates, and accelerates island formation. However, at increased growth temperature, the processes of re-evaporation, dissociation and re-sputtering of atoms from the substrate are also enhanced, resulting a degradation of the crystal quality. Therefore, the surface condition of the substrates plays a key role in the deposition of InN films, due to its low dissociation temperature at the low pressures specific to PVD processes.

The aim of this work is to study the influence of the deposition time and growth temperature on InN films deposition rate, crystallographic structure and band-gap, when deposited by reactive magnetron sputtering on un-etched (100) Si wafers, with no intermediate buffer layer.

2. Experimental

InN films were obtained in a magnetron sputtering system (AJA-Int. ATC ORION), with a base pressure less than 7×10^{-6} Pa. The metallic In cathode (99.999% purity), was sputtered in pure N₂ atmosphere, using a 13.56 MHz RF generator, delivering 100 W to the cathode. The pressure was measured in the deposition chamber with an absolute MKS 626 Barocel capacitance manometer. The substrates temperature was measured by a thermocouple and was maintained constant at a certain value in the range 350⁰-550 °C, with an accuracy of ± 5 °C.

(100) Si wafers used as substrates were chemically cleaned in an ultrasonic bath with isopropyl alcohol. No HF etching for removing the native oxide layer on Si wafer was done. Before starting films deposition, the metallic target surface was pre-sputtered for 10 min in Ar atmosphere. The substrates were biased at - 1 kV to be cleaned by Ar^+ bombardment, for additional 10 minutes, while the shutter of the magnetron was closed, to avoid any impurification.

Two sets of samples were deposited in N_2 atmosphere, for 30 and 60 minutes respectively, at a constant total pressure of 0.2 Pa, while the substrates temperature was varied the range 350 °C – 550 °C. In Table 1 are presented the deposition conditions: deposition time τ and the substrate temperature T_s at which the film growth takes place.

The XRD measurements have been performed using a Bruker-D8 Advance type X-ray diffractometer, equipped with a Cu target X-ray tube, and a scintillation detector. For thin film accurate measurements, a parallel beam geometry at grazing incidence $\alpha = 2^\circ$ in $2\theta/\theta$ scan mode was used, with a Göbel mirror in the incident beam. An asymmetric channel cut installed after the mirror provided a strictly monochromatic $\text{CuK}\alpha_1$ primary X-ray beam. Band-gap values were determined at room temperature by photoluminescence (PL), using a Horiba Jobin-Yvon HR-800 Raman spectrophotometer equipped with an excitation 632 nm HeNe laser in normal incidence mode. Film thickness was measured with a Veeco's Dektak 150 surface.

Table 1. Deposition conditions for InN films.

Sample	τ (min)	T_s [°C]
S1	30	350
S2	60	350
S3	30	450
S4	60	450
S5	30	500
S6	60	500
S7	30	550
S8	60	550

3. Results and discussion

The first observation was that for a substrate temperature higher than 550°C no film was practically deposited, due to the dissociation of InN at low pressures. The temperature threshold value for this to happen is pressure dependent, accordingly to literature data [16].

Fig. 1 shows the variation of the deposition rate with the substrate temperature, for the two deposition durations τ . The deposition rate can be clearly seen to increase with the substrate temperature – at which film growth takes place, a maximum being reached at 500°C, with the same trend for either 30 min or 60 min deposition time, as it has also been reported in the literature [17]-[18].

From Fig. 1 it clearly results that for temperatures not exceeding 500 °C, the deposition rate is higher for the shorter deposition period. This fact is due to the progressive coverage of the In target with the synthesis

product InN, which has a lower sputtering yield, as compared to metallic In [19]. A further increase of the deposition temperature, from 500 °C to 550 °C, determines an abrupt decrease of the deposition rate, as InN dissociation starts to compete with film growth [18].

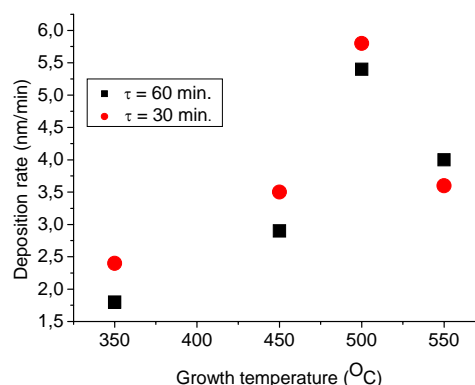


Fig. 1. Variation of the deposition rate with the deposition temperature, for different deposition periods τ .

For 550 °C substrate temperature, in contrast with the data obtained at lower temperatures, the higher deposition rate was obtained for $\tau = 60$ min, and was probably due to the relatively low thermal conductivity of InN films [20], exhibiting values comparable to alumina [21], which, in the longer term, is lowering the average temperature at the film surface below that of the substrate, decreasing the dissociation rate and favoring the film growth processes.

The X-ray diffraction profiles of the investigated InN samples deposited at different temperatures in the range 350 °C – 550 °C, for different time periods τ are shown in Fig. 3. The XRD maxima were identified according to JCPDS card no. 050-1239 for the hexagonal InN phase (P63mc group), corresponding to the following planes: (100) at 29.14° , (002) at 31.4° , (102) at 33.1° , (101) at 43.3° , (110) at 51.6° and (103) at 57° . The shape of the diffraction lines is typical for the hexagonal structure of InN. There are evidenced sharp and symmetric reflections at 31.4° for the basal plane, accompanied by broad and asymmetric reflections for the non-basal planes (100), (101), (103) and (110). This clearly indicates a polycrystalline film, with the c-axis oriented perpendicular to the surface for all crystalline domains. [22].

From the presented XRD patterns it also results that only the hexagonal InN phase is formed, with no trace of cubic phase (JCPDS card no. 01-070-2563). The line width was corrected for instrumental broadening using a corundum reference sample. The calculated lattice parameter values, presented in Table 2, are in good agreement with the reference data for the hexagonal structure of InN ($a_{\text{JCPDS-050-1239}}=3.5378\text{Å}$; $c_{\text{JCPDS-050-1239}}=5.7033\text{Å}$). Table 2 also shows the mean crystallite size (D) determined via the Scherrer formula from the (002) line, with peak broadening being attributed only to the crystallite size effect. In Table 2 are also presented the FWHM values, as measured from the (002) line,

illustrating the direct proportionality between the films' crystallinity and their deposition time, even on Si substrates, compatible with current microelectronics manufacturing facilities.

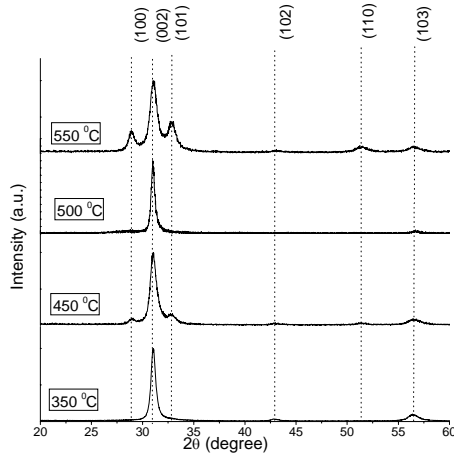


Fig. 2. XRD pattern of InN films deposited at different substrate temperatures, for $\tau=30$ min.

From Figs. 2 and 3 it can be observed that the films' crystallographic structure is changing, the films becoming more textured along the basal plane, as the deposition time increases. This may be due to the rearrangements taking place during growth, as the films become thicker. It is easily observed that the films grown at 500 °C for 60 minutes present a crystallographic structure exhibiting only one maximum corresponding to the diffraction on the basal plane. We note that the other deposition temperatures determine the apparition of multiple diffraction lines, but their intensity tends to decrease as the films thickened. This indicates that, as expected, for thicker films the characteristics of the substrate seems to have a smaller influence on the films crystalline structure.

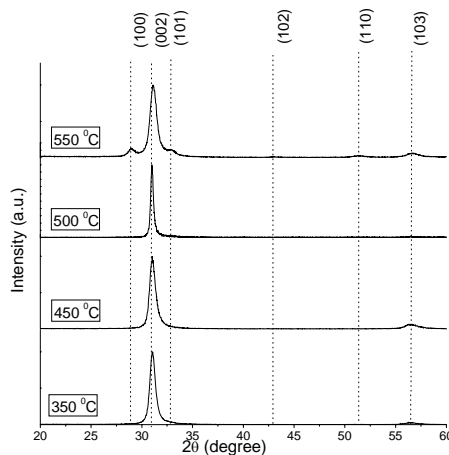


Fig. 3. XRD pattern of InN films deposited at different substrate temperatures, for $\tau = 60$ min.

Figs. 4 show the variation of the crystallite size with the deposition temperature. The crystallites size is continuously increasing with the growth temperature till 500 °C, followed by a sudden decrease. This behavior is clearly observed for both growth durations, and is ascribed to InN dissociation process taking place at this temperature.

Table 2. Lattice parameters of the deposited InN and FWHM values, as derived from (002) X-ray diffraction line.

Sample	$\langle a \rangle$ [Å]	$\langle c \rangle$ [Å]	FWHM [2 θ deg.]
S1-30	3.5577±0.0075	5.7218±0.0100	0.511
S2-4	3.5435±0.0011	5.7115±0.0021	0.640
S3-27	3.5521±0.0033	5.7307±0.0042	0.688
S4-13	3.5409±0.0036	5.7278±0.0057	0.648
S5-37	3.5080±0.0136	5.7590±0.0168	0.405
S6-38	3.5290±0.0018	5.7673±0.0026	0.297
S7-29	3.5434±0.0048	5.7252±0.0098	0.791
S8-16	3.5352±0.0008	5.7084±0.0090	0.721

For all the deposition temperatures, except for 500 °C, the crystallites seem to be a little bit larger in thinner films. However, for the highly crystalline films grown at 500 °C, a large difference in the size of the crystallites could be observed, the larger crystallites being associated with the highly textured (002) films deposited for 60 min. This means that in these deposition conditions, the mobility of the as deposited atoms/ions on the film surface is high enough to allow the formation of large crystallites which exhibit a preferred orientation perpendicular to the basal plane of the hexagonal structure, as dictated by the minimum surface energy. This deposition temperature seems to be optimal for obtaining both a high deposition rate and high crystallinity films.

For the highest growth temperature (550 °C), the crystallites size is decreasing abruptly, even below the initial values obtained for the films grown at 350 °C.

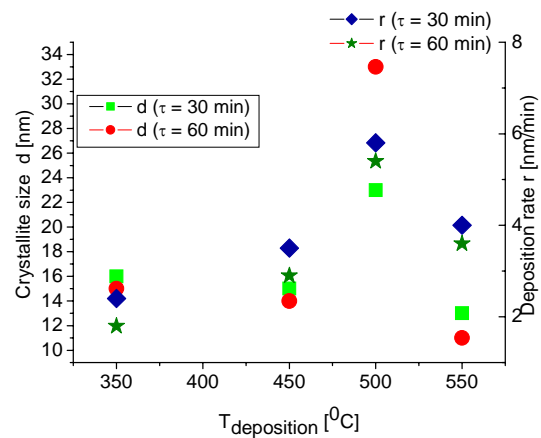


Fig. 4. Variation of the crystallite size and deposition rate with the deposition temperature.

The small size of the crystallites developed in the films grown at 550 °C could be explained by the formation of larger, polycrystalline grains, between which the cohesion would be weaker than between the crystalline domains which they are composed of.

The overall trend of the observed variations with the deposition temperature of the deposition rate and crystallite size is similar for the two deposition durations, being the result of the dynamic equilibrium between the growth and dissociation processes taking place during InN deposition.

All the samples exhibit a strong photoluminescence (PL) effect at room temperature, around 1.6 eV, slightly dependent on the deposition conditions. Figure 5 shows the PL spectra of the sample S2 and S8. It has been suggested [2] that the observed high values of the band-gap may result from quantum confinement effects related to the films polycrystalline nature. Although this hypothesis cannot be dismissed, the presence of quantum confinement effects hasn't been positively identified in InN thin films. There are other plausible explanations for low band-gap values (defects, non-stoichiometry, film non-uniformity and Mie scattering), as well as for high band-gap values (strong Moss–Burstein effect, oxygen inclusion, quantum size effects and stoichiometry changes), but neither one can describe the wide range of observed values. This might be an indication that they are due to structural features, which are depending on the growth method. The obtained band-gap value is between the 1.5-2.1 eV values reported for other films obtained by the same method [1], [23]-[25], and the small, less the 1 eV, values obtained for MBE grown films [2], [26]-[27]. This shift toward smaller values is not surprising, given the films aforementioned preferred orientation.

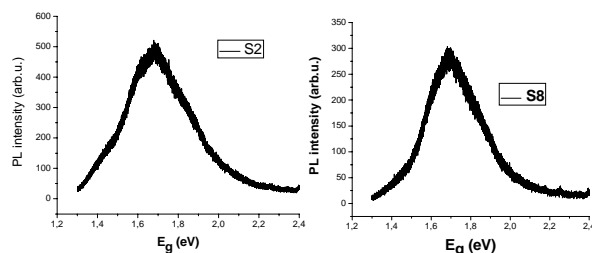


Fig. 5. Photoluminescence spectra of S2 and S8 samples.

4. Summary and conclusions

Indium nitride thin films have been deposited directly onto un-etched Si wafers without nucleation buffer by reactive RF magnetron sputtering method in nitrogen atmosphere. The films are polycrystalline with a hexagonal structure, exhibiting a preferred (002) orientation. At low deposition time multiple diffraction lines appeared, but their intensity tends to decrease as the deposition time increased. The band gap values derived from PL measurement at room temperature were around 1.6 eV, practically independent of the substrate

temperature or deposition time, being in good agreement with the values determined for other films obtained by the same method. Using a highly reproducible method, compatible with current microelectronics manufacturing facilities, we obtained InN films with characteristics suitable for use in various applications, from THz generators to microwave devices.

Acknowledgements

The work was supported by Romanian Ministry of Education and Research - MInNA Project no. 72-162/2008.

References

- [1] T. L. Tansley, C. P. Foley, *J. Appl. Phys.* **59**, 3241 (1986).
- [2] V. Yu. Davydov, A. A. Klochikhin, R. P. Seisyan, V. V. Emtsev, S. V. Ivanov, F. Bechstedt, J. Furthmuller, H. Harima, A.V. Mudryi, J. Aderhold, O. Semchinova, J. Graul, *Phys. Stat. Sol. (B)* **229**, R1 (2002).
- [3] J. Wu, W. Walukiewicz, K. M. Yu, J. W. Ager III, E. E. Haller, H. Lu, W. J. Schaff, Y. Saito, Y. Nanishi, *Appl. Phys. Lett.* **80**, 3967 (2002).
- [4] T. Matsuoka, H. Okamoto, M. Nakao, H. Harima, E. Kurimoto, *Appl. Phys. Lett.* **81**, 1246 (2002).
- [5] S. Strite, H. Morkoc, GaN, AlN, and InN: A review, *J. Vac. Sci. Technol. B* **10**, 1237-1252H (1992).
- [6] T. Egawa, H. Ishikawa, T. Jimbo, M. Umeno, *Appl. Phys. Lett.* **69**, 830 (1996).
- [7] S. Nakamura, M. Senoh, S. Nagahama, N. Iwase, T. Yamada, T. Matsushita, H. Kiyoku, Y. Sugimoto: *Jpn. J. Appl. Phys.* **35**, L74 (1996).
- [8] I. Akasaki, S. Sota, H. Sakai, T. Tanaka, M. Koike, H. Amano: *Electron. Lett.* **32**, 1105 (1996).
- [9] E. Starikov, P. Shiktorov, V. Gružinskis, L. Reggiani, L. Varani, J. C. Vaissière, H. Zhao: *Physica B* **314**, 171 (2002).
- [10] E. Starikov, P. Shiktorov, V. Gružinskis, L. Reggiani, L. Varani, J. C. Vaissière, H. Zhao: *Materials Science Forum* **384**, 205 (2002).
- [11] Knobel, A; Aidam, R; Cimalla, V, et al., *Physica Status Solidi C: Current Topics in Solid State Physics*, **6/6**, 1480 (2009).
- [12] Ahn, H; Pan, CL, *IEEE Photonics Global at Singapore, (IPGC)*, **1 - 2**, 121 (2008).
- [13] H. Shinoda, N. Mutsukura, *Thin Solid Films*, **503**, (1-2), 8-12 (2006).
- [14] X. H. Ji, S. P. Lau, H. Y. Yang, Q. Y. Zhang, *Thin Solid Films* **515**, 4619 (2007).
- [15] N. C. Zoita, L. Braic, C. Grigorescu, L. Nedelcu, *J. Optoelectron. Adv. Mater-Rapid Commun.* **2**(11), 719 (2008).
- [16] K. S. A. Butcher, T. L. Tansley, *Superlattices and Microstructures* **38**, 1 (2005).
- [17] F. Li, D. Mo, C. B. Cao, L. Choy, *Journal of Material Science: Materials in Electronics*, **12**, 725 (2001).

- [18] H. Shinoda, N. Mutsukura, *Thin Solid Films* **476**, 276 (2005).
- [19] K. Kubota, Y. Kobayashi, K. Fujimoto, *Journal of Applied Physics*, **66**(7), 2984 (1989).
- [20] S. Krukowski, A. Witek, J. Adamczyk, J. Jun, M. Bockowski, I. Grzegory, B. Lucznik, G. Nowak, M. Wróblewski, A. Presz, *Journal of Physics and Chemistry of Solids*, Volume 59, Issue 3, March 1998, Pages 289-295].
- [21] R. G. Munro, *Journal of the American Ceramic Society*, **80**, 1919 (1997).
- [22] N. Takahashi, H. Sugiura, T. Nakamura, M. Yoshioka, *Solid State Sciences* **6**, 383 (2004).
- [23] F. E. Fernandez, E. Rodriguez, M. Pumarol, T. Guzman, W. Jia, A. Martinez, *Thin Solid Films* **377**, 781 (2000).
- [24] T. Yodo, H. Ando, D. Nosei, Y. Harada, *Phys. Status Solidi b* **228**, 21 (2001).
- [25] T. Yodo, H. Yona, H. Ando, D. Nosei, Y. Harada, *Appl. Phys. Lett.* **80**, 968 (2002).
- [26] T. Miyajima, Y. Kudo, K.-L. Liu, T. Uruga, T. Honma, Y. Saito, M. Hori, Y. Nanishi, T. Kobayashi S. Hirata, *Phys. Status Solidi, B Basic Res.* **234**, 801 (2002).
- [27] Y. Nanishi, Y. Saito, T. Yamaguchi, *Jpn. J. Appl. Phys.* **42**, 2549 (2003).

*Corresponding author: laurentiu_braic@inoe.ro